


# Heterogeneous Skeleton for Summarizing Continuously Distributed Demand in a Region

**Alan T. Murray**

Department of Geography, University of Santa Barbara, CA, USA


amurray@ucsb.edu

 <https://orcid.org/0000-0003-2674-6110>

**Xin Feng**

Department of Geography, University of Santa Barbara, CA, USA


xin.feng@geog.ucsb.edu

 <https://orcid.org/0000-0001-6434-3895>

**Ali Shokoufandeh<sup>1</sup>**

Department of Computer Science, Drexel University, Philadelphia, PA, USA

ashokouf@cs.drexel.edu

 <https://orcid.org/0000-0002-3729-4490>

---

## Abstract

There has long been interest in the skeleton of a spatial object in GIScience. The reasons for this are many, as it has proven to be an extremely useful summary and explanatory representation of complex objects. While much research has focused on issues of computational complexity and efficiency in extracting the skeletal and medial axis representations as well as interpreting the final product, little attention has been paid to fundamental assumptions about the underlying object. This paper discusses the implied assumption of homogeneity associated with methods for deriving a skeleton. Further, it is demonstrated that addressing heterogeneity complicates both the interpretation and identification of a meaningful skeleton. The heterogeneous skeleton is introduced and formalized, along with a method for its identification. Application results are presented to illustrate the heterogeneous skeleton and provides comparative contrast to homogeneity assumptions.

**2012 ACM Subject Classification** Applied computing → Operations research, Information systems → Geographic information systems, Theory of computation → Computational geometry

**Keywords and phrases** Medial axis, Object center, Geographical summary, Spatial analytics

**Digital Object Identifier** 10.4230/LIPIcs.GIScience.2018.12

## 1 Introduction

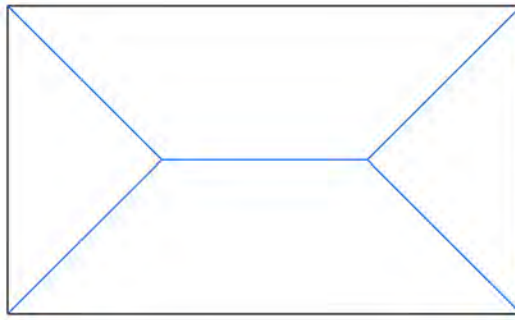
An area, polygon and/or region is often the byproduct of political, administrative or management delineation, but such an object can also be used to represent in situ phenomena and attributes. Irrespective of its origin, summary, explanation and characterization of the spatial extent of an area-based object can be very important. One approach for summary representation has been through the use of the skeleton, or medial axis among other names. Okabe et al. [16] note the ability of the skeleton to characterize the shape of a polygon. In cartography, the skeleton may be used for effective label placement, contributing to visual appeal and enhanced communication of a display and/or map. Bruck et al. [5] and Matisziw

---

<sup>1</sup> Ali SHokoufandeh's work supported in part by the National Science Foundation under Grant Number PFI:AIR-TT:1640366.



## 12:2 Heterogeneous Skeleton



■ **Figure 1** Skeleton for a rectangle region.

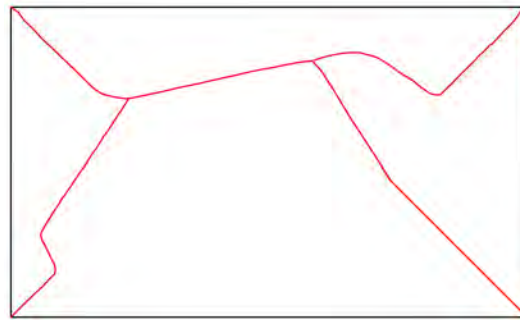


■ **Figure 2** Heterogeneous attribute for the rectangle region.

and Murray [14] have demonstrated important spatial properties of the skeleton, as have others.

The skeleton is a line-based object that is represented by the locus of all points equidistant to at least two nearest locations on the polygon boundary it describes. Figure 1 depicts the skeleton (colored blue) for a rectangle region (colored black). Interestingly, definition of the skeleton has focused only on the polygon boundary, devoid of any other spatial attributes. In particular, one might consider an attribute distributed within a polygon as an important influencing factor, if such information is available. It may be that only the total value of an attribute for a polygon is known, and not its actual spatial distribution within the polygon. We know the total attribute value within the rectangle region in Figure 1 to be 58,217. Clearly in such a case, the standard definition based on polygon boundary makes sense. However, if the spatial attribute distribution within a polygon is indeed known, then this should influence the shape of the skeleton if it is to reflect both boundary and attribute information. Figure 2 depicts the spatial variability of the attribute in the rectangle region (Figure 1), where darker colors correspond to higher attribute values (greater population). The 58,217 people in this region are not uniformly distributed, but rather are non-uniform, with a high of 40 people in the left top corner cell and a low of one in right bottom corner cell. One can characterize the skeleton based only on polygon boundary as homogeneous, whereas a skeleton based on boundary and spatially varying attribute(s) within the polygon would be better described as heterogeneous. Figure 3 depicts the heterogeneous skeleton for the rectangle region, accounting simultaneously for both boundary and attribute variability.

In this paper we introduce the heterogeneous skeleton to simultaneously reflect boundary and attribute variability of a polygon. The idea is to provide enhanced summary and characterization, taking advantage of the greatest amount of information possible. The



■ **Figure 3** Skeleton accounting for boundary and spatial attribute variability in rectangle region.

next section provides background on the skeleton. This is followed by technical details of homogeneous and heterogeneous skeletons. An approach for deriving the heterogeneous skeleton is given. Application results demonstrating the utility of the heterogeneous skeleton are then provided. The paper ends with discussion and concluding comments.

## 2 Background

The skeleton was identified as an efficient model for two-dimensional closed shape representation by Blum [2], and later generalized by Millman [15] and Yodmin [23]. The skeleton was also extended to curves defined by bi-tangent spheres known as the symmetry set [12, 3]. Assuming the existence of a radial function at every skeletal point, the skeleton transform is an invertible function, in that it is possible to reconstruct a shape as the union of overlapping bi-tangent spheres centered at skeletal points [10]. The skeleton also provides a concise representation for the interior of the shape, and as such is subject to both geometric and mechanical operations, including interior deformations and wrappings. It also provides a basis for shape characterization at multiple spatial scales, enabling efficient geometric processing. In terms of applications, the skeleton has played critical roles in GIScience, including topography, cartography, analytics and network modeling. For example, the structure of watersheds can be characterized by a “flooding” propagation from sources that are constrained by surface topography. This flooding operator is similar to Blum’s grassfire operator and is estimated using a similar computational approach [20]. In digital modeling, the skeleton has been used for extracting and characterizing elongated geographic structures, such as roads and rivers [1]. In cartography and mapping skeletons have been used to estimate tightly coupled level heights of contour curves to regenerate terrain models [13], but also for label placement/layout. In sensor network optimization, planning the routing for static nodes in a geometric space is a critical problem [11]. Bruck et al. [5] used skeletons to optimize routing. Matisziw and Murray [14] showed that the skeleton represents locations in continuous space having the most desirable siting properties. The skeletal representation has also been used in the context of two- and three-dimensional shape representation and recognition [13, 19]. For these problems, the skeletal representation is computed directly for the object boundary curves or surfaces and contains the topological information about shape in terms of the local descriptors, which are held at each node in the skeletal representation [9]. These local shape descriptors contain information to aid shape retrieval, matching, and analysis [7, 18].

The (homogeneous) skeleton represents a line-based object center, and was characterized above as being the locus of all points equidistant to at least two nearest locations on the polygon boundary. Consider the polygon shown in Figure 4. The challenge is to identify



■ **Figure 4** A polygon-based region,  $\Phi$ .

a line-based object that is a summary of this polygon. The skeleton represents one such approach.

A set theoretic model for the skeleton can be structured. Assume we have a simple polygon object,  $\Phi$ . Further, this polygon can be converted to its polyline representation,  $\varphi$ . Both objects are now used in the characterization of the skeleton:

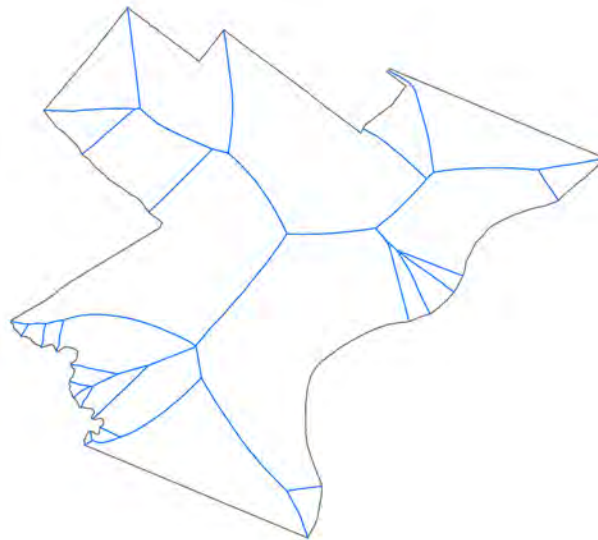
$$S = \left\{ p \in \mathbf{R}^2 \mid \forall r \in \mathbf{R}, \left( \delta(p, r) \subset \Phi \right) \wedge \left( |\delta(p, r) \cap \varphi| \geq 2 \right) \right\} \quad (1)$$

where  $p$  is a point in two-dimensional space,  $r$  is a distance (Euclidean), and  $\delta(p, r)$  is a polyline object (circle) of distance  $r$  from point  $p$ . The skeleton results from an infinite collection of instances of  $p$  and  $r$ , where  $\delta(p, r)$  is contained in  $\Phi$  and  $\delta(p, r)$  intersects  $\varphi$  in two or more tangent points. Further discussion of the skeleton can be found in Okabe et al. [16] and Matisziw and Murray [14].

Given this formal specification of the skeleton, it may be derived using a number of methods. There are different approaches that have been well documented for skeleton extraction of two- and three-dimensional objects. They can be grouped into three major categories based on their principles and object representation:

1. Voronoi - Algorithms based on the Voronoi diagram or continuous geometric approaches of point clouds, polygonal, or polyhedral representations of object boundaries. Based on properties of the Voronoi diagram, Voronoi edges or planes can be used to construct symmetry structures, or the skeleton.
2. Thinning - Algorithms that rely on the continuous evolution of object boundaries. For example, the object boundary is shrunk with the spread of fire starting at the boundary, the so called grassfire algorithm. The skeleton is formed at the location of singularities, referred to as the “quench points” where fires from different parts of the boundary meet.
3. Distance transformation - Algorithms using the principle of digital morphological erosion or location of singularities, e.g., local maxima, on a digital distance transform field.

Figure 5 illustrates the associated skeleton for polygon  $\Phi$  shown in Figure 4. As noted previously, the skeleton is the byproduct of evaluation that considers only polygon boundary. As a result, there are no attribute oriented influences in the structure of the skeleton.



■ **Figure 5** Homogeneous skeleton of polygon  $\Phi$ .

### 3 Heterogeneous Skeleton

A polygon region that has associated attribute detail about variability within it represents a rich source of information. While a standard assumption is to assume that a polygon attribute is uniformly distributed across the area it delineates, when ancillary information exists regarding the actual spatial distribution of an attribute, this is particularly valuable. The skeleton,  $S$ , defined using (1) assumes homogeneity and is derived solely on the basis of polygon boundary  $\varphi$ . Yet, more may be known about attribute variability, and this has the potential to provide greater spatial richness to a line-based summary. As an example, Figure 6 indicates population density for the study region. Darker shades indicate higher population density, and it is clearly not uniform across the polygon. Extending the skeleton/medial axis to account for both geographic boundary as well as heterogeneity in the distribution of attributes across  $\Phi$  is important.

This means then that one must be able to explain and account for attribute variability. In continuous space the function  $g()$  defines the attribute value for any point  $q \in \mathbf{R}^2$ .

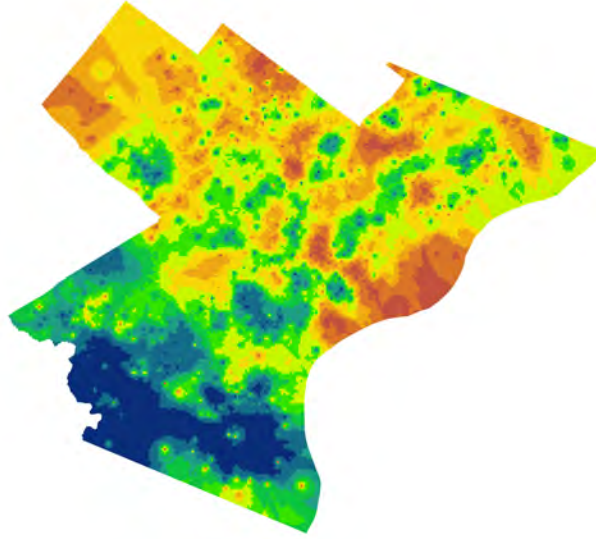
Using set theory notation, we introduce the heterogeneous skeleton as:

$$W = \left\{ \rho^* \in \mathbf{R}^2 \mid \forall p \in \mathbf{R}^2, r \in \mathbf{R}, \left( \delta(p, r) \subset \Phi \right) \wedge \left( |\delta(p, r)| \cap \varphi \geq 2 \right) \right. \\ \left. \wedge \min_{\rho^*} \iint_{q \in \delta(p, r)} g(q) \gamma(\rho^*, q) dq \right\} \quad (2)$$

where  $\gamma(\rho^*, q)$  is the distance between  $\rho^*$  and  $q$ . Building on the homogeneous skeleton,  $S$ , definition in (1), the heterogeneous skeleton in (2) adds the additional condition that the inscribed circle,  $\delta(p, r)$ , serves as an object for which the best representative point is sought. This representative point then helps to define the proposed skeleton variant.

The subproblem communicated in (2) is:

$$\min_{\rho^*} \iint_{q \in \delta(p, r)} g(q) \gamma(\rho^*, q) dq \quad (3)$$



■ **Figure 6** The attribute variability within region  $\Phi$ .

This is actually a continuous space optimization problem (see Church and Murray [6]). A discrete variant of (3) is what Rogerson [17] and others refer to as the weighted median center. With demand in  $\delta(p, r)$  distributed according to the function  $g(\cdot)$ , the distance  $\gamma(\rho^*, q)$  from point  $q$  to the optimal median center  $\rho^*$  reflects the weighted distance. That is, we seek the optimal  $\rho^*$  for each inscribed circle,  $\delta(p, r)$ , such that the total weighted (attribute) distance is minimized. It therefore is the most efficient or most representative center point for  $\delta(p, r)$ . The collection of optimal  $\rho^*$  for all points  $p \in \mathbf{R}^2$  satisfying (2) results in the heterogeneous skeleton.

Often the attribute function  $g(\cdot)$  is approximated in some way (Yao and Murray [22]), where  $\delta(p, r)$  is delineated into smaller reporting units or cells. The index  $i$ ,  $i \in \{1, \dots, n\}$ , is used to refer to discrete points/units in  $\delta(p, r)$ , where  $(x_i, y_i)$  are the coordinates of unit  $i$ . Naturally,  $g_i$  represents the observed attribute value for unit  $i$ . If the coordinates of  $\rho^*$  are  $(X, Y)$ , then these are the subproblem decision variables. The weighted median center is therefore the following problem:

$$\min_{(X, Y)} \sum_{i=1}^n g_i \sqrt{(x_i - X)^2 + (y_i - Y)^2} \quad (4)$$

The distance function,  $\gamma(\cdot)$ , in this case is the Euclidean metric. As noted in Wesolowsky [21] and Church and Murray [6], (4) is nothing other than the Weber problem and can be solved using the Weizfeld algorithm.

With the problem description and details, an approach to solve (2) is possible. Pseudo code for the solution process is as follows:

Effectively, the proposed approach must first identify each inscribed circle, as done for  $S$  in (1). However, the point to include on the heterogeneous skeleton, denoted as  $W$  in (2), is defined based upon the weighted median center criteria, (4). Depending on the structure of polygon  $\Phi$ , as the number of  $\rho^*$  defining  $W$  increases, the associated heterogeneous skeleton results.

---

**Algorithm 1** Overview of heterogeneous skeleton derivation.
 

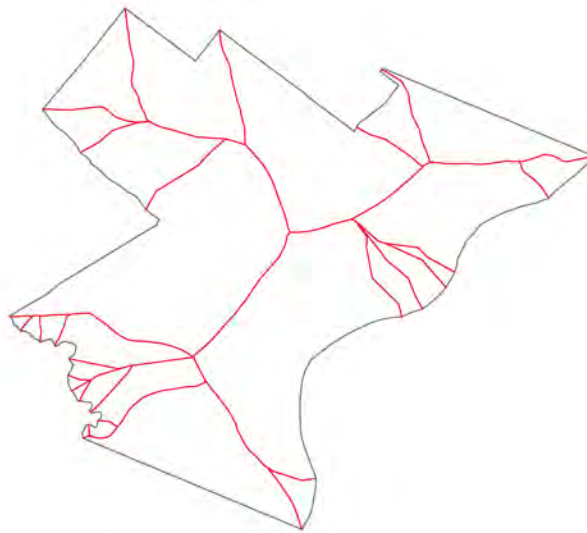
---

```

for  $\delta(p, r)$  in  $\Phi$  do
   $\delta(p, r) \subset \Phi$ 
   $|\delta(p, r) \cap \phi| \geq 2$ 
  Find  $\rho^*$ , or rather  $(X, Y)$  using (4)
end for

```

---



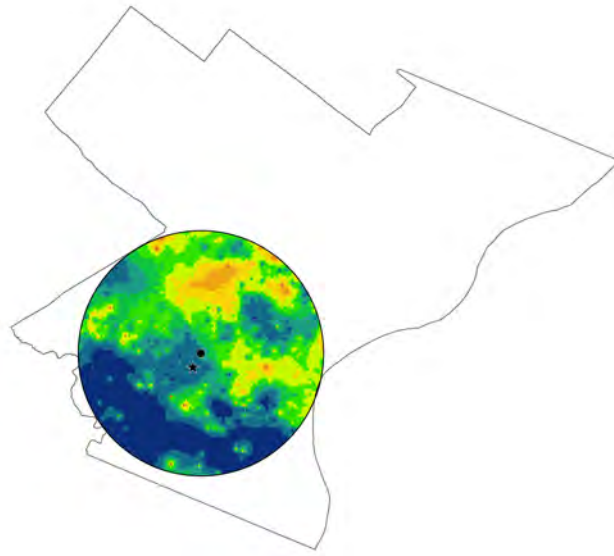
■ **Figure 7** Heterogeneous skeleton (boundary and attribute variability).

## 4 Results

The models were implemented in the Python platform using `arcpy`, `pysal` and `sympy` libraries, among others, on a Windows 10 Enterprise server with an Intel Xeon E5-2650 v3 (2.3GHz) 64 bit CPU and 64 GB of RAM. ArcGIS was utilized for data creation, management, manipulation, analysis, and visualization. Reported findings required only seconds or minutes to derive.

The heterogeneous skeleton is shown in Figure 7 for the study region (Figures 4 and 6). In comparison to the homogeneous skeleton (Figure 5), there is much variability in the line-based object in terms of precisely where the skeletal line segments are located. The reason for this is highlighted in Figure 8, where an inscribed circle is depicted,  $\delta(p, r)$  and helps to form the derived skeleton. The unweighted median center is shown using the symbol  $\bullet$ . This is the feature which is used to define the homogeneous skeleton,  $S$ , in equation (1). In contrast, the weighted median center, (4), is shown using the symbol  $\star$ . That is what is being used to define the heterogeneous skeleton,  $W$ , in equation (2). Accordingly, the two skeletons are different based upon their resulting line segments. This happens because of the added influence of attribute and its spatial variability, i.e., the higher population density areas are effectively pulling the skeleton to create a shape and location that is more representative of the distribution of the underlying attribute.

One final question to consider is how distinct the heterogeneous and the classic homogeneous skeletons are. While visual inspection and comparison highlights significant differences, aspects of quantification are possible. One distinction can be made in terms of how far apart



■ **Figure 8** Inscribed circle with associated attribute variability.

the unweighted and weighted median center are from each other for each inscribed circle used in defining the skeleton. In this case, the distance between the homogeneous center and the corresponding heterogeneous center ranges from 3.43 to 3,593.07 ft in this case. The mean distance is 1220.54 ft, with a standard deviation 939.55 ft. As the region is nearly 100 square miles, such differences are highly significant.

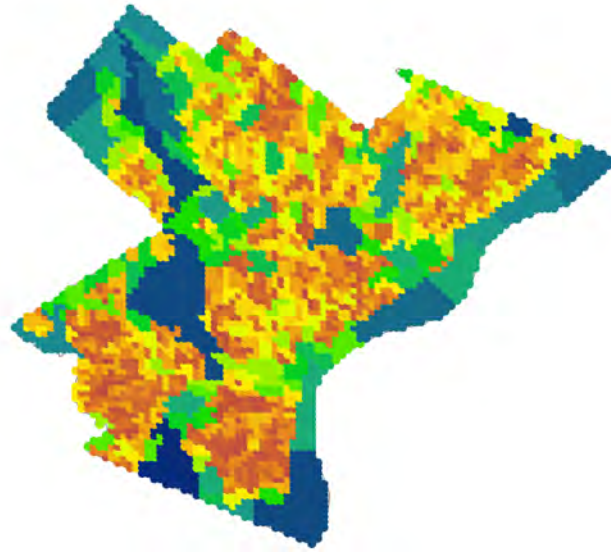
## 5 Discussion and Conclusions

There are a number of issues worth further investigation associated with the heterogeneous skeleton. First, a polygon may have many possible associated heterogeneous skeletons, one for each one of its attributes. For example, if there are  $m$  attributes referenced using  $j \in \{1, \dots, m\}$ , then any unit  $i$  would have  $m$  unique attribute values  $g_{ij}$ . As a result, depending on the spatial variability of the attribute, one could anticipate  $m$  unique heterogeneous skeletons that reflect attribute variation along with the influence of boundary footprint. Figure 9 illustrates a second attribute for polygon  $\Phi$ , with a decidedly different pattern of spatial variability. Figure 10 indicates the associated skeleton in this case. As is evident through visual inspection, the skeleton in Figure 10 is much different from the case where population is considered (Figure 7). Thus, many different heterogeneous skeletons may be possible depending on associated spatial attributes.

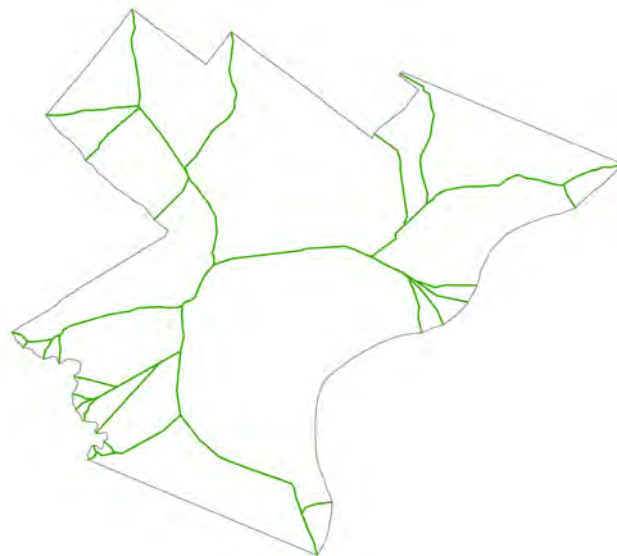
The derivation of the heterogeneous skeleton detailed here was based on the notion of inscribed circles,  $\delta(p, r)$ . Here, the main motivation was to maintain a connection to the original construction of skeletal representation. This also ensures that one can account for boundary and attribute variability. While this is theoretically sound, other definitions of the heterogeneous skeleton too may be appropriate and meaningful. It is conceivable that approaches based on modified differential grassfire operators or distance transform may be mathematically intuitive or computationally more efficient [8, 4].

The paper introduced the heterogeneous skeleton to help simultaneously characterize boundary and attribute variability of a polygon-based region. The classic definition of a skeleton was reviewed, highlighting the focus on the defining boundary only. Taking into





■ **Figure 9** Second regional attribute.



■ **Figure 10** Second regional attribute.

account attribute information in the formalization of the skeleton has many potential benefits given the wide array of already established application areas. In particular, the heterogeneous skeleton represents an approach for summarizing multi-dimensional information that includes both spatial detail as well as locational attributes. The work here represents an initial attempt to define and derive the heterogeneous skeleton.

---

#### References

- 1 Sylvain Airault, Oliver Jamet, and Frederic Leymarie. From manual to automatic stereoplotting: evaluation of different road network capture processes. *International Archives of Photogrammetry and Remote Sensing*, 31:14–18, 1996.

- 2 Harry Blum. A transformation for extracting new descriptors of shape. *Models for Perception of Speech and Visual Forms, 1967*, pages 362–380, 1967.
- 3 Gunilla Borgefors. On digital distance transforms in three dimensions. *Computer vision and image understanding*, 64(3):368–376, 1996.
- 4 Heinz Brey, Joseph Gil, David Kirkpatrick, and Michael Werman. Linear time euclidean distance transform algorithms. *IEEE Transactions on Pattern Analysis and Machine Intelligence*, 17(5):529–533, 1995.
- 5 Jehoshua Bruck, Jie Gao, and Anxiao Jiang. Map: Medial axis based geometric routing in sensor networks. *Wireless Networks*, 13(6):835–853, 2007.
- 6 Richard L Church and Alan T Murray. *Business Site Selection, Location Analysis, and GIS*. Wiley, 2009.
- 7 Christopher M Cyr and Benjamin B Kimia. 3d object recognition using shape similarity-based aspect graph. In *Computer Vision, 2001. ICCV 2001. Proceedings. Eighth IEEE International Conference on*, volume 1, pages 254–261. IEEE, 2001.
- 8 James Damon. Smoothness and geometry of boundaries associated to skeletal structures i: sufficient conditions for smoothness (la lissité et géométrie des bords associées aux structures squelettes i: conditions suffisantes pour la lissité). In *Annales de l'institut Fourier*, volume 53, pages 1941–1985, 2003.
- 9 M Fatih Demirci, Ali Shokoufandeh, and Sven J Dickinson. Skeletal shape abstraction from examples. *IEEE Transactions on Pattern Analysis and Machine Intelligence*, 31(5):944–952, 2009.
- 10 Eric Ferley, Marie-Paule Cani-Gascuel, and Dominique Attali. Skeletal reconstruction of branching shapes. In *Computer Graphics Forum*, volume 16, pages 283–293. Wiley Online Library, 1997.
- 11 Stefan Funke. Topological hole detection in wireless sensor networks and its applications. In *Proceedings of the 2005 joint workshop on Foundations of mobile computing*, pages 44–53. ACM, 2005.
- 12 Peter J Giblin and SA Brassett. Local symmetry of plane curves. *The American Mathematical Monthly*, 92(10):689–707, 1985.
- 13 Benjamin B Kimia, Allen R Tannenbaum, and Steven W Zucker. Shapes, shocks, and deformations i: the components of two-dimensional shape and the reaction-diffusion space. *International journal of computer vision*, 15(3):189–224, 1995.
- 14 Timothy C Matisziw and Alan T Murray. Area coverage maximization in service facility siting. *Journal of Geographical Systems*, 11(2):175–189, 2009.
- 15 David Milman. The central function of the boundary of a domain and its differentiable properties. *Journal of Geometry*, 14(2):182–202, 1980.
- 16 Atsuyuki Okabe, Barry Boots, Sugihara Sugihara, Kokichi, and Sung Nok Chiu. *Spatial Tessellations: Concepts and Applications of Voronoi Diagrams, second condition*. John Wiley & Sons, 2000.
- 17 Peter A Rogerson. *Statistical Methods for Geography: a student's guide, fourth edition*. Sage, 2015.
- 18 Ali Shokoufandeh, Diego Macrini, Sven Dickinson, Kaleem Siddiqi, and Steven W Zucker. Indexing hierarchical structures using graph spectra. *IEEE Transactions on Pattern Analysis and Machine Intelligence*, 27(7):1125–1140, 2005.
- 19 Kaleem Siddiqi, Juan Zhang, Diego Macrini, Ali Shokoufandeh, Sylvain Bouix, and Sven Dickinson. Retrieving articulated 3-d models using medial surfaces. *Machine vision and applications*, 19(4):261–275, 2008.
- 20 Luc Vincent and Pierre Soille. Watersheds in digital spaces: an efficient algorithm based on immersion simulations. *IEEE Transactions on Pattern Analysis & Machine Intelligence*, 13(6):583–598, 1991.

- 21 George O Wesolowsky. The weber problem: history and perspectives. *Location Science*, 1(1):5–23, 1993.
- 22 Jing Yao and Alan T Murray. Continuous surface representation and approximation: spatial analytical implications. *International Journal of Geographical Information Science*, 27(5):883–897, 2013.
- 23 Yosef Yomdin. On the local structure of a generic central set. *Compositio Math*, 43(2):225–238, 1981.